Extended electron states and magnetotransport in a 3-simplex fractal

Arunava Chakrabarti*
Max-Planck-Institut für Physik Komplexer Systeme, Nöthnitzer Strasse 38, D-01187 Dresden, Germany
(Received 21 June 2005; revised manuscript received 19 August 2005; published 28 October 2005)

We perform a real space renormalization group analysis to study the one electron eigenstates and the transmission coefficient across a 3-simplex fractal lattice of arbitrary size, in the presence of a magnetic field. In particular, we discuss the existence of extended electronic states and the influence of the magnetic field on the spectrum of the system. A general formulation is presented which enables us to deal with both the isotropic and the anisotropic cases. It is found that, in general, the transmission across an anisotropic fractal is larger than its isotropic counterpart. Additionally, we point out an interesting correlation between a subset of values of the external field, and the multiple fixed point cycles of the Hamiltonian corresponding to the extended eigenstates. A prescription for observing such a correlation is proposed. This aspect may be important in the classification of the extended states in such deterministic structures.

DOI: 10.1103/PhysRevB.72.134207 PACS number(s): 61.44.−n, 71.23.An, 72.15.Rn, 73.20.Jc

I. INTRODUCTION

The physics of noninteracting electrons on lattices without any translational invariance has been the subject of intense theoretical activity for many years. Beginning with the work of Anderson[1] describing the absence of diffusion in randomly disordered lattices, a wealth of knowledge has now accumulated in this field. Over the last couple of decades the problem of electron localization in low-dimensional quasi-crystalline[2] and fractal lattice models[3–17] have enriched this field further.

Rammal and Toulouse[3] have discussed the spectral features of several deterministic fractal models, which have also been studied with an analysis of the density of states, distribution of the eigenvalues, and the character of eigenfunctions by Domany *et al.*[4] In particular, Domany *et al.*[4] have introduced a recursive scheme for such an analysis, and have pointed out that in some deterministic fractals such as the Sierpinski gasket, the allowed energy values group into two classes with respect to the gap intervals. One group of energy values lies inside the gaps, and the other values constitute the gap edges. Schwalm and Schwalm,[5,8] and Schwalm *et al.*[7] have addressed the important problem of conductance in a fractal lattice using a Green's function formalism, and the real space rescaling method. The corner-to-corner propagation in a set of deterministic fractals has been shown to exhibit interesting behavior. From the superlocalization theory we know that on choosing an energy randomly within the spectrum, the Kubo-Greenwood conductance sum goes to zero faster than an exponential decay.[9,10] Nevertheless, there are energies for which the conductance of a class of deterministic fractal lattices exhibits a power law dependence on the system size,[5–8] the scaling exponent revealing a multifractal distribution in the thermodynamic limit. However, there are energies for which the conductance remains constant and independent of the lattice size in certain cases. In fact, the number of such states is uncountably infinite, and of measure zero.[5–8] The behavior of the conductance in a set of deterministic fractals has been discussed in detail by Schwalm and Schwalm elsewhere.[11]

Regular fractal networks have already been proposed to be used to model the principal geometric features of the backbone of the percolation clusters.[12,13] Such systems, by the way they are generated, are self-similar and exhibit the absence of any long range translational order. Yet they are not random. This gives the fractal networks the status of being intermediate between perfectly periodic structures and completely disordered ones. Naturally, they became the objects of detailed theoretical study over all these years.

A regular fractal lattice with finite ramification (meaning that a large part can be detached by removing a finite number of bonds) is generally solvable, and is found to possess exotic spectral features, some of which have already been highlighted above. The properties are similar for electrons and other excitations such as phonons or magnons. Contrary to the absolutely continuous electronic spectrum of a perfectly crystalline sample, or the pure point spectrum of a randomly disordered lattice, the electronic spectrum of a deterministic fractal is typically a Cantor set of measure zero.[4] However, referring back to the works by Rammal and Toulouse,[3] and by Domany *et al.*,[4] one finds that there also exists an infinite set of isolated energies in the gaps of the Cantor set spectrum, which corresponds to the so-called "molecular localized states." The changing local environment around each lattice[14] point leads to localization of the single particle eigenstates, but in a way not found common in conventional disordered samples. The conductance in such fractalline systems is also found to show up power-law scaling with the size of the system, as we have already mentioned.

Deterministic fractal lattices are also found to support extended eigenstates, though the presence of a continuum of extended eigenstates is yet to be proved. The general characteristics of such states are already discussed in Ref. 3,4. The influence of such states on the conductance of fractal lattices is extensively discussed using the Green's function formalism and the renormalization group methods by Schwalm and Schwalm.[15,16] Later, other authors also pointed out extended single particle states in certain deterministic fractal lattices.[17–19] The existence of extended eigenstates in a fractal is interesting, as such a lattice does not have translational invariance, neither does it possesses any short ranged "positional correlation" between the lattice points, as in the cases of certain random or quasi-periodic lattice models.[20–23]

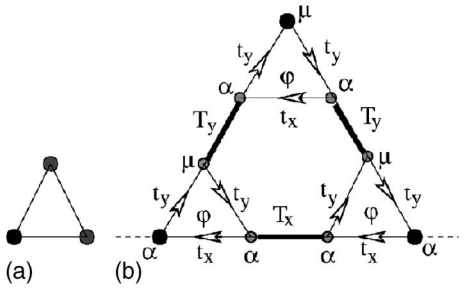

FIG. 1. (a) The basic building block of a 3-simplex network. (b) The lattice in its second generation. The dotted lines indicate the leads attached for transmission studies.

In the latter systems, local "atomic" clusters cause resonance at certain electron energies, leading to a perfect transmission, and extended single particle states.[20–23] No such local clusters of sites can really be identified in the conventional deterministic fractals. The delocalization of an infinite number of extended single particle states in a fractal can thus be attributed to the structure of the lattice as a whole.

In this communication we report a real space renormalization group (RSRG) analysis of the spectral features of a 3-simplex fractal[24] in the presence of a constant magnetic field. The growth of a 3-simplex fractal is described in Fig. 1. We choose the magnetic flux to penetrate the small triangular plaquettes at each generation, in a direction perpendicular to the plane of the fractal. This results in a break in the time reversal symmetry as the electron hops along the edges of a basic triangle. The hopping along the "bond" joining the two neighboring triangle remains unaffected by the field. The magnetic field is already known to have a nontrivial effect on the Cantor set energy spectrum usually supported by such fractals as has been demonstrated in the case of a Sierpinski gasket network.[3,25,26] The degeneracy of the zero field solution is found to be broken, and the energy spectrum broadens up, though the isolated character of the eigenstates is preserved. Later, Wang[27] re-examined the Sierpinski gasket in the presence of a magnetic field using an RSRG method, but allowed only a subset of the full parameter space to evolve under RSRG transformations. The suppression of the evolution of the full parameter space, to our mind, sometimes may lead to incomplete information about the eigenstates.

We take up the investigation of the spectral properties of a 3-simplex lattice mainly motivated by the following ideas. First, apart from being representatives of certain percolation clusters, deterministic fractal geometries have also been realized experimentally. Modern nanofabrication techniques have made it possible to experimentally investigate model systems, such as the Josephson junction arrays and superconducting networks developed following a Sierpinski gasket fractal[28,29] where both the nature, and the amount of disorder, can be accurately controlled. The level of frustration in such a case can be tuned by an external magnetic field. Additionally, recent experimental measurements of persistent current in an array of mesoscopic rings[30] suggest that one can think of a deterministic fractal network with multiple loops at all scales of length and observe the interplay of magnetic field and the fractal geometry in the transport and related issues in such networks. A study in this regard has already received some attention,[31] but deserves more analysis.

Second, and a major objective is that we wish to take a deeper look at whether the external magnetic field, if it generates extended eigenfunctions for the fractal, is linked to any cyclic invariance of the Hamiltonian. If such cycles at all exist, it is important to understand whether they have any correlation with the values of the external flux responsible for them. In that case it would be possible to tune the flux, which is an external *agent* to control the transport in finite fractal networks, as well as a classification between diffrent extended states could be achieved. This aspect which has remained, to the best of our knowledge, unexplored so far, is a major focus of the present work.

We find several interesting features. In the absence of any field, and with the introduction of anisotropy in the amplitude of electron hopping, the corner-to-corner transmission of a 3-simplex fractal turns out to be better than its isotropic counterpart. Clusters of high transmittivity pack the transmission spectrum in the former case, whereas the system turns out to be poorly transmitting in the isotropic situation. This remains the general feature for both the isotropic and the anisotropic cases when a magnetic field is turned on, with the transmission coefficient exhibiting interesting Aharonov-Bohm (AB) oscillations.

The magnetic field is also found to have a dramatic effect on the local density of states at a corner site of an infinite (or semi-infinite) 3-simplex fractal. An apparently continuous distribution of eigenvalues appear around the center of the spectrum, suggesting the formation of a band of extended states. We have not been able to prove conclusively the existence of a band of extended states. However, extensive numerical investigations of the local density of states and the behavior of the nearest neighbor hopping integrals under renormalization group iterations are suggestive of the fact. An important observation in this regard is that recently, Schwalm and Moritz[32] have done extensive analysis on a family of hierarchical lattices. They[32] report that the spectra of the model Hamiltonian for certain finitely ramified hierarchical lattice turn out to be continuous with smooth local density of states. Using a renormalization group method, they have shown that the Greenwood-Peierls conductance at certain energy shows a metallic behavior rather than tending to zero with increasing lattice size.

Finally, we have focused on a specific value of the energy of the electron which supports an extended eigenstate only in the presence of a magnetic flux, and have carried out careful numerical investigations on the flow of the parameters of the Hamiltonian under repeated renormalization of the system, as the flux is changed systematically. We find that, for this specific extended eigenstate, values of the magnetic flux show a strong correlation with the fixed point cycles of the parameter space that can be predicted successfully. Such observations may provide an idea of classifying the extended states in regard of the fixed points of the Hamiltonian brought about by the external magnetic field.

In what follows, we report our results. In Sec. II, we introduce the model and the RSRG scheme. Section III contains a discussion on the nature of the energy spectrum both

in the absence and the presence of a field. Section IV is devoted to the investigation of magnetotransport, while in Sec. V we discuss how the flux values can be correlated to the cycles of the fixed point. In Sec. VI we draw our conclusions.

II. THE MODEL AND THE RSRG SCHEME

We begin by referring to Fig. 1. The three basic triangular plaquettes [Fig. 1(a)] are placed as shown in the figure to generate a second-generation fractal [Fig. 1(b)]. The process continues. A magnetic field penetrates each small triangle. We work within a tight binding formalism in which the Hamiltonian for the electron in a basic triangular plaquette is written as

$$H = \sum_i \epsilon_i c_i^\dagger c_i + \sum_{\langle ij \rangle} t_{ij} e^{i\theta} c_i^\dagger c_j \tag{1}$$

In the above, ϵ_i is the on site potential which, in the most general anisotropic model, can assume two values, ϵ_α (at the corner sites at the horizontal base of each elementary triangle) and ϵ_μ at the remaining vertices. The nearest neighbor hopping integrals t_{ij} are assigned amplitudes t_x and t_y for hopping across the horizontal and the angular bonds within each elementary triangle, respectively. The intertriangle connection is given by $t_{ij}=T_x$ in the horizontal direction, and $t_{ij}=T_y$ otherwise, as depicted in Fig. 1(b), and these are free from any associated flux. It is to be appreciated that the status of a vertex (α or μ) is governed only by the bonds t_x or t_y attached to it. T_x and T_y remain undecimated on renormalization and do not play a part in fixing the status of a vertex. It may also be noted at this point that this 3-simplex network differs, in the presence of a magnetic field penetrating its elementary plaquettes, from its closest lookalike the Sierpinski gasket[27] by the fact that in the 3-simplex network, the time reversal symmetry of the electron hopping is broken only partially, i.e., when the electron hops along the edges of an elementary triangle, compared to a Sierpinski gasket where it is broken uniformly. It will be interesting to see the consequence of this at various scales of length. Before we launch into the details, it is important to make a note of the fact that the spectrum of a model self-similar fractal has previously been studied by Rammal and Toulouse,[3] and by Alexander.[25] The nesting property of the eigenvalues, related to the Z_3 symmetry of a Sierpinski gasket has been critically discussed in the former using a Sierpinski gasket as an example, while Alexander[25] treats the same lattice using a Green's function formalism. Using the implicit symmetry of the lattice the spectrum of the $n+1$ stage gasket is shown to be related to that of the nth stage. Alexander provides a proof of the Rammal-Toulouse nesting property as well.[25] We now move on to describe the present work.

The magnetic flux threading each small triangle enters the Hamiltonian only through the hopping integrals along the sides of the elementary triangles.[26] We set $\theta=2\pi\Phi/(3\Phi_0)$. Here, Φ is the flux threading each small triangle, and Φ_0 is the flux quantum. Following Banavar, Kadanoff, and Pruisken,[26] we select the gauge in such a way that the a factor of $\exp(i\theta)$ is associated with either t_x or t_y when the electron hops in the direction given by the arrow. The phase is opposite when it hops back. Thus, the forward or the backward hopping integrals in the presence of the field will be written as $t_{x(y)}^{F(B)}=t_{x(y)}e^{\pm i\theta}$. The model, as it is presented, allows one to study a general anisotropic case ($t_x \neq t_y$), including a hierarchical distribution of the bonds T_x or T_y, which is known to exhibit interesting "restoration of isotropy" in a 3-simplex network of classical resistors,[33] although, we do not pursue this topic here. The isotropic limit is easily retrieved as well.

The sites marked with decorated circles in Fig. 1(b) are decimated to yield the following recursion relations for the on-site potentials and the hopping integrals.

$$\epsilon_{\alpha,n+1} = \epsilon_{\alpha,n} + C_{1,n} t_{y,n}^F + D_{1,n} t_{x,n}^B \tag{2}$$

$$\epsilon_{\mu,n+1} = \epsilon_{\mu,n} + C_{4,n} t_{y,n}^B + D_{4,n} t_{y,n}^B$$

$$t_{x,n+1}^F = C_{3,n}^* t_{y,n}^B + D_{3,n}^* t_{x,n}^F$$

$$t_{y,n+1}^F = C_{2,n} t_{y,n}^F + D_{2,n} t_{x,n}^B$$

$$t_{x,n+1}^B = t_{x,n+1}^{F\,*}$$

$$t_{y,n+1}^B = t_{y,n+1}^{F\,*}$$

In the above, n and $n+1$ in the subscript denote the stages of renormalization, $t^{F(B)}{}_{j,n} = t_{j,n}e^{\pm i\theta_n}$ with $j=x$ or y representing the x or y hopping along the edge of a triangle, and, θ_n is the renormalized flux at the nth stage, which we do not have to calculate separately. Here

$$C_{1,n} = \frac{A_{1,n} + A_{2,n}B_{1,n}}{1 - A_{2,n}B_{2,n}}$$

$$C_{2,n} = \frac{A_{3,n} + A_{2,n}B_{3,n}}{1 - A_{2,n}B_{2,n}}$$

$$C_{3,n} = \frac{A_{4,n} + A_{2,n}B_{4,n}}{1 - A_{2,n}B_{2,n}}$$

$$C_{4,n} = \frac{B_{5,n} + A_{5,n}B_{6,n}}{1 - A_{6,n}B_{6,n}} \tag{3}$$

$$D_{1,n} = \frac{B_{1,n} + B_{2,n}A_{1,n}}{1 - A_{2,n}B_{2,n}}$$

$$D_{2,n} = \frac{B_{3,n} + B_{2,n}A_{3,n}}{1 - A_{2,n}B_{2,n}}$$

$$D_{3,n} = \frac{B_{4,n} + B_{2,n}A_{4,n}}{1 - A_{2,n}B_{2,n}}$$

$$D_{4,n} = \frac{A_{5,n} + B_{5,n}A_{6,n}}{1 - A_{6,n}B_{6,n}}$$

At any stage n of renormalization, we have defined (suppressing the subscript n) $A_1 = rt_y^B/s$, $A_2 = (rt_y^F + T_x T_y^2 t_x^B t_y^B)/s$, $A_3 = T_y(qt_y^F + pt_y^B t_x^B)/s$, $A_4 = T_y^2 t_x^B[(E-\epsilon_\alpha)t_y^F + t_x^B t_y^B]/s$, $A_5 = t_y^B z_1/[z_1(E-\epsilon_\alpha) - T_y^2]$, $A_6 = (z_1 t_x^F + v_1 T_y t_y^B)/[z_1(E-\epsilon_\alpha) - T_y^2]$, and $B_1 = t_x^F/z$, $B_2 = (rt_y^B + T_x T_y^2 t_x^F t_y^F)/(rz)$, $B_3 = uT_x T_y t_y^F/(pz)$, $B_4 = T_x[wT_y t_y^F + t_x^B(E-\epsilon_\mu) + (t_y^F)^2]/(pz)$, $B_5 = t_y^F/z_2$, and $B_6 = (T_y w_2 + t_x^B)/z_2$.

The quantities u, w, z, v_1, z_1, w_2, and z_2 are defined as

$$u = \frac{p[t_x^F(qt_y^F + pt_y^B t_x^B) + rt_y^B]}{qr} \tag{4}$$

$$w = \frac{T_y[t_x^B t_y^B + (E-\epsilon_\alpha)t_y^F]}{qr}(pt_x^F t_x^B + r)$$

$$z = (E-\epsilon_\alpha) - \frac{T_x[(E-\epsilon_\mu)T_x + t_y^F T_y v]}{p}$$

with, $v = [pT_x T_y t_x^F t_x^B t_y^B + rT_x T_y t_y^B]/(qr)$,

$$v_1 = \frac{T_x T_y t_y^B}{p(E-\epsilon_\alpha) - T_x^2(E-\epsilon_\mu)}$$

$$z_1 = (E-\epsilon_\mu) - w_1 t_y^B \tag{5}$$

with, $w_1 = t_y^F p/[p(E-\epsilon_\alpha) - T_x^2(E-\epsilon_\mu)]$, and,

$$w_2 = \frac{(t_y^F)^2 T_x T_y}{(E-\epsilon_\mu)[p(E-\epsilon_\alpha) - T_x^2(E-\epsilon_\mu)] - pt_y^F t_y^B} \tag{6}$$

$$z_2 = (E-\epsilon_\alpha) - T_y v_2$$

with

$$v_2 = \frac{T_y[p(E-\epsilon_\alpha) - T_x^2(E-\epsilon_\mu)]}{(E-\epsilon_\mu)[p(E-\epsilon_\alpha) - T_x^2(E-\epsilon_\mu)] - pt_y^F t_y^B}$$

.

Finally, the remaining factors are

$$p = (E-\epsilon_\alpha)(E-\epsilon_\mu) - t_y^F t_y^B$$

$$q = (p - T_y^2)(E-\epsilon_\alpha)$$

$$r = q(E-\epsilon_\alpha) - pt_x^F t_x^B \tag{7}$$

$$s = r(E-\epsilon_\mu) - qT_y^2.$$

The intertriangle hopping integrals T_x and T_y remain unaffected as a result of renormalization, i.e., $T_{j,n+1} = T_{j,n}$ at any stage n, with j representing x or y.

The set of recursion relations given by Eq. (2) is a highly nonlinear one, and can be reduced to a simple form only under simple isotropic model in the absence of any field. However, they are not so difficult to deal with numerically, and yield quite a few interesting results which we shall now discuss.

III. ENERGY SPECTRUM AND THE NATURE OF EIGENSTATES

A. The zero field case

To begin with, we have evaluated the local density of states (LDOS) at a corner site of a 3-simplex gasket in the isotropic limit and in the absence of any magnetic field. We set $\epsilon_\alpha = \epsilon_\mu = \epsilon$, $t_x = t_y = t$, and $T_x = T_y = \tau$. The recursion relations given by Eq. (2) now get reduced to

$$\epsilon_{n+1} = \epsilon_n + \frac{P_n}{Q_n R_n}$$

$$t_{n+1} = \frac{U_n}{Q_n R_n} \tag{8}$$

with $P_n = 2t_n^2[(E-\epsilon_n)^2 - \tau(E-\epsilon_n) - t_n^2]$, $Q_n = (\tau + t_n + \epsilon_n - E)$, $R_n = \tau^2 - (E-\epsilon_n)^2 + t_n^2 - \tau t_n$, and $U_n = \tau t_n^2(E-\epsilon_n + t_n - \tau)$; n again stands for the stage of renormalization. In the absence of any field, it is a simple task to evaluate the LDOS at a corner site using the standard Green's function technique.[34] We have checked that the recursion relations produce the correct LDOS at the corner site of a one-dimensional chain[35] in the limit t_y, $T_y \to 0$. With a small imaginary part added to the energy E, the hopping integral t flows to zero after certain steps of RSRG. This implies that the lattice, at that scale of length, breaks up into an assembly of diatomic molecules, with the hopping τ connecting the atoms remaining unchanged. Each such molecule will be decoupled from its neighbors, and the transmission across the lattice will be zero. The on-site potential at the corner site reaches its fixed point value $\tilde{\epsilon}$, and, the LDOS (meaningful only at an extreme corner site, which is truly decoupled from the rest of the lattice) is then evaluated as

$$\rho(E) = -\frac{1}{\pi}\mathrm{Im}[G_{00}(E + i\eta)] \tag{9}$$

where the diagonal Green's function $G_{00} = 1/(E - \tilde{\epsilon})$. A plot of the LDOS at a corner site is shown in Fig. 2 (top figure). The LDOS exhibited is checked, as permitted by the limit of accuracy, to be stable against a decreasing value of the imaginary part of the energy E, and has been displayed within a value unity to give prominence to the smaller peaks compared to the much larger ones. The fragmented, scanty appearance is consistent with the usual Cantor set spectrum common to such systems. We end this paragraph by noting that Hood and Southern[36] have also studied the density of states of an anisotropic Sierpinski gasket. The spectrum is found to be composed of two distinct parts—localized molecular modes and hierarchical modes. Interestingly, with the onset of anisotropy, they find that the localized modes disappear and only the hierarchical modes remain in the spectrum.

Before introducing the magnetic field, it is pertinent to comment on the existence of extended eigenstates in this simplified model. If the recursion relations in Eq. (8) are iterated for any arbitrary energy with no imaginary part added to it, the hopping integral t flows to zero after certain steps of RSRG. This means that the corresponding energy should lie in a gap of the spectrum of the infinite system, or

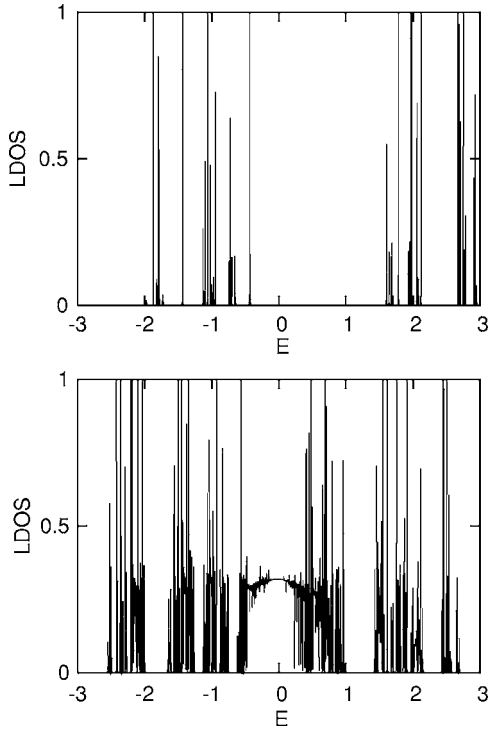

FIG. 2. The local density of states at a corner site of an isotropic 3-simplex fractal. The top figure corresponds to the case of zero flux, whereas the bottom one corresponds to the case where the flux $\Phi=\Phi_0/4$. We select $\epsilon=0$ and $t=1$. The imaginary part added to the energy is 10^{-5} in units of t.

corresponds to an exponentially localized eigenstate, though it is not possible to distinguish between these two cases by simply looking at the flow of the hopping integral. It should be remembered that a zero LDOS is not a conclusive proof for an energy not to be in the spectrum of the infinite lattice. On the other hand, if, for certain energy, the hopping integral remains nonzero under an indefinite number of iterations, then we have definitely hit upon an extended eigenstate. It is not difficult using Eq. (8) to fix an energy for which $\epsilon_1=\epsilon$. The energy, evaluated in this fashion, can then be inserted into the second equation in Eq. (8), and one can select τ in such a manner that t_1 under RSRG remains equal to t. As the intertriangle hopping is always τ, we thus have a fixed point of the parameter space, viz, $(\epsilon_n, t_n, \tau_n) \rightarrow (\epsilon_{n-1}, t_{n-1}, \tau_{n-1})$ for $n \geqslant 1$. The corresponding state will be extended in nature. This demands a definite relationship between ϵ, t, and τ, that is, we are talking about a specific model. For example, with $\epsilon=0$ and $t=1$, if we set $E=0.5t$, then the fixed point behavior sets in from the first RSRG step onward if τ is assigned a value equal to $-3/2$ (in units of t). A more involved relationship between the parameters of the system is capable of leading to a fixed point behavior starting at deeper scales of renormalization. However, in each case, a different set of parameters essentially means that we are dealing with a different system. In principle, we will observe extended eigenstates in each of those cases which provide a meaningful relationship between the parameters, but only at certain discrete energy values.

B. A magnetic field is turned on

A magnetic field, however, is capable of bringing dramatic changes into the spectrum even when we deal with a particular system with a predefined set of parameters. In the lower part of Fig. 2 the LDOS at the corner site is shown for a flux $\Phi=\Phi_0/4$ for the simplest isotropic model with $\epsilon_\alpha=\epsilon_\mu=0$ and $t_x=t_y=T_x=T_y=1$. The spectrum shows very closely spaced zones of finite density of states. Of particular interest is the narrow energy interval around the center $E=0$, where the appearance of a smooth region of almost constant density of states exits. It has not been possible to prove the existence of a continuous *band* of states, though we have made a very fine scan around $E=0$, each time reducing the energy interval to be scanned and diminishing the imaginary part to be added to the energy E. The LDOS is found to be stable under a variation in the imaginary part η from 10^{-3} to 10^{-10} (in units of t) and within the limits of machine accuracy, it is tempting to conjecture the existence of a continuous zone of eigenstates around $E=0$. The occurrence of dense clusters of nonzero density of states has been tested with other values of the magnetic field. The general conclusion is the same (except for $\Phi=m\Phi_0/2$, with m being an integer), and the qualitative features do not essentially change even when we deal with the anisotropic gasket.

IV. TRANSMISSION ACROSS FINITE 3-SIMPLEX FRACTALS

To calculate the quantum mechanical transmission across a finite 3-simplex network of any size, we adopt the well known formalism proposed by Stone *et al.*,[37] and consequently used by others as well.[19] The essential method consists in placing the desired fractal network between perfectly ordered semi-infinite leads [shown by dashed lines in Fig. 1(b)] connected to the two extreme α-sites at the base. The leads may be described by a uniform on-site potential ϵ_0 and constant nearest neighbor hopping integral t_0. A network at the nth generation is then renormalized $n-1$ times to reduce it to a simple triangle, and finally to a diatomic molecule[19] still clamped between the leads, with an effective on-site potential ϵ_{eff}, and an effective hopping integral $t_{eff}^{F(B)}$. The transmission coefficient is then easily obtained in terms of the quantities ϵ_{eff}, $t_{eff}^{F(B)}$, ϵ_0, t_0, and the electron energy E. The method is so well known that we skip the detailed mathematical expressions to save space and present the results only.

A. Zero flux situation

Let us start with the isotropic case, that is, $\epsilon_\alpha=\epsilon_\mu$ and $t_x=t_y=T_x=T_y$. Consider no flux, i.e., $\Phi=0$. The transmission spectrum consists of the expected isolated peaks, consistent with the LDOS spectrum. With increasing size, the fractal turns out to be poorly transmitting. Interesting changes start showing up with the introduction of anisotropy. Quite arbitrarily, we set $t_x=T_x=1$ and start reducing the values of $t_y(=T_y)$ from one toward zero (the limit when the fractal reduces to a linear chain clamped between the leads). The on-site potentials ϵ_α and ϵ_μ are chosen to be equal, and have

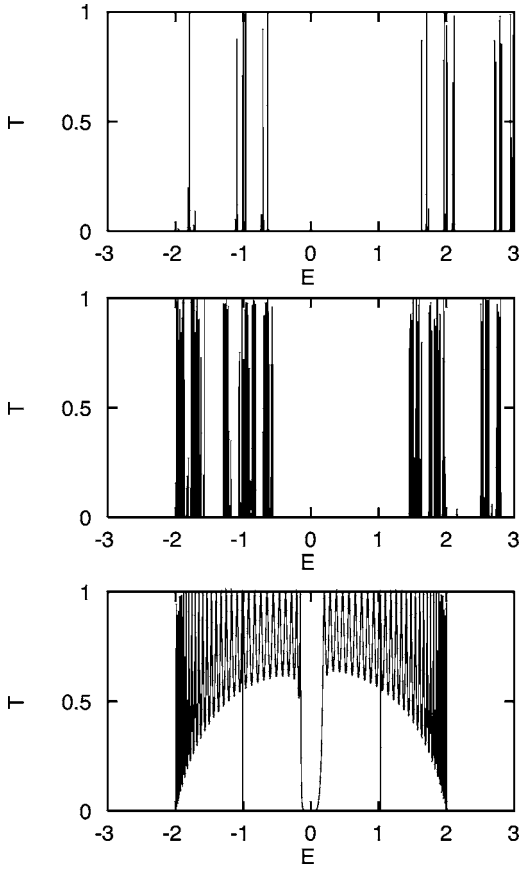

FIG. 3. The transmittivity (T) against energy of a seventh generation 3-simplex fractal. The top figure corresponds to the isotropic case with $t_x=t_y=T_x=T_y=1$. The middle and the bottom ones depict the situation with $t_y=T_y=0.9$ and $t_y=T_y=0.1$, respectively. The on site potentials are kept constant at $\epsilon_\alpha=\epsilon_\mu$ in each case. The lead parameters are $\epsilon_0=0$ and $t_0=2$.

been set equal to zero. With the introduction of anisotropy, regions of finite transmission increase in number. For example, putting $t_y=T_y=0.9$ (that is, a small departure from isotropy), the spectrum is still very much like the isotropic situation, with new clusters of appreciable transmittance (sometimes unity as well) appearing in many places. With gradual decrease in the values of the y hopping, the newly generated small spiky zones increase in number, join "hand in hand" and the shape of the entire spectrum starts drifting toward what it should be in the case of a periodic chain clamped between the leads. The spectrum tends to be restricted within $E=\epsilon_0\pm 2t_0$, which is the allowed band of the ordered lead, and resembles the spectrum of a 1d chain as $t_y=T_y$ becomes vanishingly small. In Fig. 3 we show the transmission spectrum of a seventh generation 3-simplex structure, both for the isotropic situation (top) and the anisotropic cases (the middle and bottom ones) in support of the above remarks.

B. Influence of the magnetic field

We have investigated the general features of the transmission coefficient as the flux through each elementary plaquette

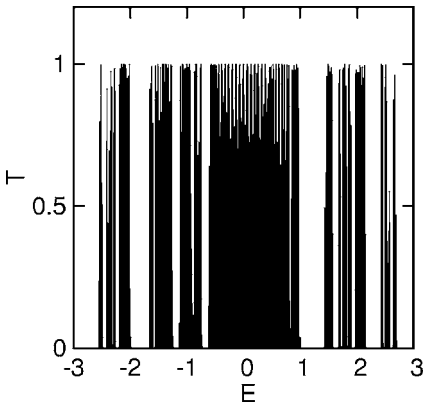

FIG. 4. The transmittivity (T) against energy of a sixth generation 3-simplex fractal. The figure corresponds to the isotropic case with $t_x=t_y=T_x=T_y=1$. The on site potentials are kept constant at $\epsilon_\alpha=\epsilon_\mu=0$ and the magnetic flux threading each elementary triangular plaquette is $\Phi=\Phi_0/4$. For the lead, we take $\epsilon_0=0$ and $t_0=2$.

is varied. The features are, of course sensitive, to the energy of the electron that enters the system through the lead. For calculation we have chosen $\epsilon_\alpha=\epsilon_\mu=0$ and $t_x=T_x=t_y=T_y=1$. The lead parameters in this case are chosen to be $\epsilon_0=0$ and $t_0=2$ to encompass the full spectrum of the fractal network. In the case of an isotropic 3-simplex network, the magnetic field is found to generate clusters of resonant transmission throughout the spectrum, a particularly noticeable broadening taking place at and around $E=0$. In Fig. 4 we display the transmission spectrum of a sixth generation fractal with energy E with a flux $\Phi=0.25\Phi_0$ threading each elementary triangle. The spectrum is notable for a thick population of high transmission values at and around $E=0$. Several other *mini-bands* of resonant transmission also mark the spectrum. This feature is in sharp contrast to that in the absence of any field (Fig. 3, the top figure for example). We have observed the change in the width of the cluster of high transmission zone around $E=0$ by carefully scanning the energy interval. It is seen that the width of the transmission window around $E=0$, for any generation, changes continuously with the introduction of the flux, from zero at $\Phi=0$ to a maximum at $\Phi=\Phi_0/4$, and then shrinks back to zero again at $\Phi=\Phi_0/2$. The change in width of this central transmitting window shows a periodic variation with flux. The period is equal to a half flux quantum. Similar observations as above are made with anisotropy in the hopping integrals, but with no real new qualitative features. The portion of the T and Φ/Φ_0 graph immediately around $E=0$ remains densely packed with the increasing size of the network (Fig. 3. bottom).

The second half of the study of transmission spectrum consists of an examination of the Aharonov-Bohm (AB) oscillations in the transmission coefficient at a fixed energy of the electron. We have displayed results for $E=0$. The period of oscillations is found to be equal to one flux quantum. The detailed features of the spectrum are sensitive to the chosen energy of the electron. In Fig. 5 we show the AB oscillations within one period for a third and a sixth generation gasket. Once again the transmission window between zero and one-half flux quantum shows multiple resonance peaks in the sixth generation fractal compared to a fairly broad and struc-

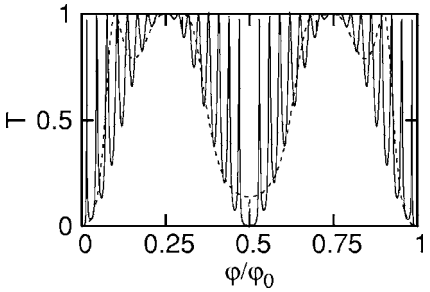

FIG. 5. The transmittivity (T) against flux of a third generation (dotted line) and a sixth generation (solid line) 3-simplex fractal. The figure corresponds to the isotropic case with $t_x=t_y=T_x=T_y=1$ and $\epsilon_\alpha=\epsilon_\mu=0$. We have set $E=0$.

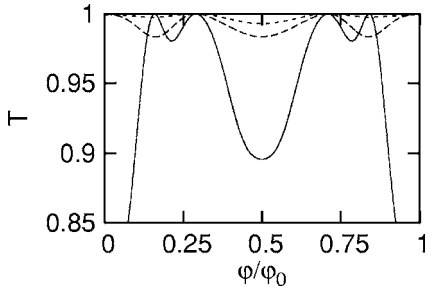

FIG. 6. The transmittivity (T) against flux of a seventh generation fractal. The figure corresponds to the anisotropic cases with $t_x=T_x=1$, $\epsilon_\alpha=\epsilon_\mu=0$ and $t_y=T_y=0.25$ (solid line); $t_y=T_y=0.20$ (dashed line) and $t_y=T_y=0.15$ (dotted line). We have set $E=0.5$ in units of t_x.

tureless shape observed in the third generation. Interestingly, with increasing generation, the spectrum is enriched by the appearance of multiple peaks with transmission equal to one (or, very close to one), but the transmittivity really does not fall to zero for any appreciable value of the flux between $0<\Phi<\Phi_0/2$ and $\Phi_0/2<\Phi<\Phi_0$.

The sensitivity of the spectral features on the parameters of the system are easily revealed when we look at the variation of the transmission coefficient against changing magnetic flux in the case of an anisotropic simplex lattice. While the electron with $E=0$ does not distinguish between an isotropic and an anisotropic fractal, other energy values may lead to gross changes in the fine structure of the spectrum. We point out an interesting phenomenon. It is possible to fix the electron energy in such a way that with large anisotropy (that is, for low enough values of $t_y=T_y$), the amplitudes of the AB oscillations start decreasing as the transmission coefficient assumes values very close to one. At one stage, the transmittance T becomes practically indistinguishable from unity, as $t_y=T_y$ is brought below certain value. By magnifying the scale of observation, it is still possible to see how the system tries to preserve the AB oscillations, which soon smoothes out if the y hopping is diminished further. In such cases, with increasing generation the hopping integral $t_{y,n}$ flows to zero, while $t_{x,n}$ does not. It means, as the system grows in size, the intricate geometry of the fractal starts "disappearing" to the incoming electron. It essentially feels an ordered chain, and if the energy chosen happens to lie in the allowed band of that ordered chain, we get a ballistic transport. In Fig. 6 we display one such example where $E=0.5$ in units of t_x.

V. FIELD INDUCED EXTENDED STATES

A. General remarks

The existence of extended eigenstates in systems without any translational order has always been an intriguing feature in the study of disordered systems. However, the complex forms of the recursion relations make an analytical attempt rather difficult for a 3-simplex network. We have therefore relied on a careful numerical study. We specially observe the flow of the hopping integrals under successive RSRG steps. The nonzero values of the hopping integrals under RSRG stand out to be a definite signature of the state being extended. In all the discussion that follows, we confine ourselves to the isotropic case only.

It is now evident that the magnetic field generates a dense set of eigenvalues, almost resembling a continuum, around $E=0$. Quite arbitrarily we have selected a portion $-0.1\leqslant E\leqslant 0.1$, in unit of t_x in a model with $\epsilon_\alpha=\epsilon_\mu=0$, $t_x=T_x=t_y=T_y=1$, and have chosen the value of the magnetic flux $\Phi=\Phi_0/4$. The LDOS in this portion is found to be very stable as the imaginary part added to the energy is decreased from 10^{-3} to 10^{-9}. A fine scan over the points in this interval reveals that any energy we hit upon quite randomly in this range corresponds to a nonzero value of the nearest neighbor hopping integral under successive renormalization. This indicates the presence of extended eigenstates. Of course, this is not a conclusive proof of the existence of a band of extended states, but the smaller and smaller widths of the energy interval chosen, remaining close to $E=0$, lead to similar behavior. This is suggestive of the presence of a band of extended eigenstates. But once again, a conclusive proof is lacking. We have carried out the numerical investigation for other values of the flux and other energy intervals, and in many occasions similar observation has been made. The observations are in accord with the transmission spectrum displayed in Fig. 5.

B. Values of flux and cycles of the fixed point: An interesting correlation

Let us now turn to a different aspect of the problem. We restrict the discussion to the isotropic model with $\epsilon_\alpha=\epsilon_\mu=\epsilon$ and $t_x=T_x=t_y=T_y=t$. The phase associated with the hopping at any nth stage of RSRG will be denoted by θ_n. We draw the attention of the reader to Fig. 7, which presents the transmission as a function of the applied flux for a seventh generation 3-simplex fractal (solid line), together with the LDOS (dashed line) at $E=0$, plotted by varying the flux from zero to a single flux quantum. It is interesting to see how the energy $E=0$ is periodically brought in and out of the spectrum of the infinite system by the magnetic field, the period being equal to $\Phi_0/2$. Once again we have tested the robustness of the LDOS spectrum by diminishing the imaginary part added to energy from larger (10^{-3}) to much smaller

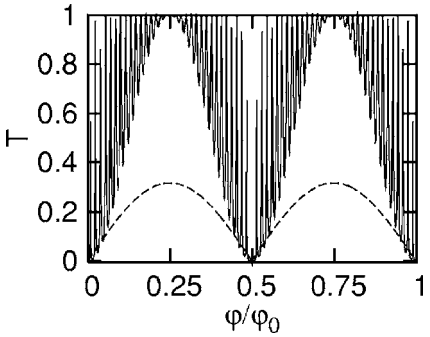

FIG. 7. The transmittivity (T) against flux of a seventh generation fractal (solid line) and the local density of states at a corner site of an infinite lattice (dashed line) at $E=0$. We address the isotropic case with $t_x=t_y=T_x=T_y=1$ and $\epsilon_\alpha=\epsilon_\mu=0$.

(10^{-9}) values, so that it is not unjustified to conclude that we definitely have a state at $E=0$. The spectrum also gives us an indication that we have a continuous LDOS as flux changes from zero to half flux quantum. We fix our energy of interest at $E=0$. Looking at the evolution of the hopping integral under successive RSRG steps as we gradually increase the flux threading an elementary triangular plaquette from zero to $\Phi_0/2$ and beyond, we make two interesting observations. First, for $0<\Phi<\Phi_0/2$ and $\Phi_0/2<\Phi<\Phi_0$, the hopping integrals do not flow to zero under iteration, bringing out the fact that $E=0$ corresponds to a perfectly extended eigenstate for what appears to be a continuous distribution of flux values.

Second, different flux values chosen for the above observation unravel the existence of fixed points with multiple cycles. Most interestingly, we have found that the values of the magnetic flux leading to these cyclic fixed points group into a definite pattern, the formation of which can be predicted from the results of our numerical scan of the range of the flux values. The same pattern (of the number of cycles) is repeated as we change the flux at certain specially chosen equal intervals along the flux line from $\Phi=0$ to $\Phi=\Phi_0/2$. We clarify the meaning of the above statements below by citing specific results.

Let us consider the interval $\Phi=0$ to $\Phi=\Phi_0/2$, and divide this interval into 2^m subintervals with m being a positive integer and $m\geqslant 2$. If we exclude the two extreme points at $\Phi=0$ and $\Phi=\Phi_0/2$ on this flux line, then the remaining values of the magnetic flux making this division are distributed at the locations (coordinates) $\Phi_j=(j/2^{m+1})\Phi_0$, $j=1,2,3,\ldots,2^m-1$. Let us pick up the simplest choice, i.e., $m=2$. The interval $0<\Phi<\Phi_0/2$ is then split into four equal subintervals. The values of the flux inside the line (that is, excluding the values at the boundary) are located at $\Phi_1=\Phi_0/8$, $\Phi_2=\Phi_0/4$, and $\Phi_3=3\Phi_0/8$, sequentially from the left. We set $\Phi=\Phi_1=\Phi_0/8$. It is immediately observed that the entire parameter space defined by the trio $(\epsilon_n,t_n,\theta_n)$ gets locked into a two-cycle fixed point beginning at $n=3$, where n represents the RSRG step. That is, we have for $\Phi=\Phi_0/8$

$$(\epsilon_n,t_n,\theta_n)=(\epsilon_{n+2},t_{n+2},\theta_{n+2}),\ n\geqslant 3.$$

With $\Phi=\Phi_2=\Phi_0/4$, we again get a two-cycle fixed point of the parameter space $(\epsilon_n,t_n,\theta_n)$. But now the fixed point behavior is observed for $n\geqslant 2$. Setting the external flux equal to the remaining value in this interval, i.e., $\Phi=\Phi_3=3\Phi_0/8$, we get a one-cycle fixed point of the same parameter space beginning at $n=1$, that is, at the first stage of RSRG onward. It should be appreciated that the values of the flux $\Phi=\Phi_0/8$ and $\Phi=\Phi_0/4$ can be termed equivalent only in the *number of cycles of the fixed point* they generate. The extended wavefunctions they represent are characteristically different as the invariant cycles of the parameter space set in at different stages of renormalization.

We now increase the value of m in steps. The behavior of the parameter space defined by $(\epsilon_n,t_n,\theta_n)$ is observed under successive RSRG iteration as the magnetic flux is made to assume sequential values given by $\Phi=(j/2^{m+1})\Phi_0$ from the left. Our experiment leads to these interesting observations. If we denote the flux leading to an n-cycle fixed point by $\Phi(n)$, then the values of the flux between zero and the half flux quantum group themselves into a series of *triplets*, i.e., $[\Phi(2),\Phi(2),\Phi(1)]$. This triplet repeats itself periodically as we sweep through the points $\Phi_j=j/2^{m+1}\Phi_0$ along the flux axis between zero and half flux quantum. For any given value of m which fixes the number of intervals, the cyclic invariance of the full parameter space will start showing up at a specific step of renormalization. This step n is given by the power m of 2 in the denominator in the expression for the flux Φ, whenever $\Phi=[(2l+1)/2^m]\Phi_0$ and $l=0,1,2,\ldots$.

Thus, for an eight subinterval splitting of the range $0\leqslant\Phi\leqslant\Phi_0/2$, the first value (after zero) at $\Phi=(1/2^4)\Phi_0$ exhibits a 2-cycle fixed point starting at $n=4$. The second flux $\Phi=(2/2^4)\Phi_0=(1/2^3)\Phi_0$ leads to a 2-cycle fixed point beginning at $n=3$. For $\Phi=(3/2^4)\Phi_0$ we have a one-cycle fixed point for $n\geqslant 4$. This sequence of cycles repeats periodically, but the stage at which the invariance starts showing up is not the same for every flux. However, for values of $m>2$, a subset of the fixed points (one cycle or two cycle) are truly equivalent in the sense that they start showing up at the same stage of RSRG. In this sense, the fixed points arising out of flux values $\Phi=\Phi_0/2^m$, $\Phi=5\Phi_0/2^m$, and $\Phi=7\Phi_0/2^m$ are truly equivalent.

It should be appreciated that the sequence of flux values responsible for a certain cyclic behavior has a deterministic feature. If we select $\Phi=(1/2^m)\Phi_0$, with $m=2,3,4,\ldots$ sequentially, then its easy to check that for all such values of Φ we have a two-cycle fixed point beginning at $n=m$. Thus, at the leftmost value of the flux, the cyclic invariance starts revealing at the deepest scale of length. As we move along the flux line, the fixed point character begins to show up earlier and at $\Phi=\phi_0/4$, we see it immediately from $n=2$ onward. Similarly, whenever $\Phi=(3p/2^m)\Phi_0$, with $p=1,2,3,\ldots$, and $m\geqslant 2$, we come across a one-cycle fixed point for $n\geqslant m$. For example, by selecting $m=5$, the values of the flux at $\Phi/\Phi_0=3/2^5$, $6/2^5=3/2^4$, $9/2^5$, $12/2^5=3/2^3$, and $15/2^5$ exhibit one-cycle fixed point beginning at $n=5$, 4, 5, 3, and 5 respectively. Similar deterministic features have also been possible to locate for other subdivisions.

It is obvious that the separation between the one-cycle and the two-cycle values of the flux becomes exponentially smaller as we split the flux interval between zero and one-half flux quantum more and more by increasing m. The be-

havior of $[\Phi(2),\Phi(2),\Phi(1)]$ is consistent with our expectation as far as we have tested. This encourages us to conclude that, speaking in terms of the one- and two-cycle fixed points, there will be a "quasi-continuous" crossover in the character of the extended eigenstates as one sweeps over the specific flux values at $\Phi_j=(j/2^{m+1})\Phi_0$ along the flux line between zero and half flux quantum.

What happens in the range $\Phi_0/2 \leqslant \Phi \leqslant \Phi_0$?

Similar correlations between the flux values and the cycles of the fixed points may also be looked for the flux ranging from $\Phi=\Phi_0/2$ to one flux quantum. The pattern however, may be different. For example, if we split the full range of flux from $\Phi=0$ to $\Phi=\Phi_0$ in $2^5=32$ equal intervals, then it is seen that from $\Phi=j\Phi_0/32$ with $j=1,2,\ldots,15$, the pattern $[\Phi(2),\Phi(2),\Phi(1)]$ is periodically repeated. The midpoint $\Phi=\Phi_0$ has to be omitted as we do not get any state there. In the rest of the flux interval, that is, from $\Phi=17\Phi_0/32$ and up to $\Phi=31\Phi_0/32$ in intervals of $\Phi_0/32$, we now get a triplet $[\Phi(2),\Phi(1),\Phi(2)]$ repeating periodically. One can proceed in this way for other values of m. For any given m, the entire pattern observed between $\Phi=0$ and $\Phi=\Phi_0$ obviously repeats beyond one flux quantum. We have tested these observations by working out the patterns for a few values of m and then speculated the pattern for larger values of m. This test has been successful and gives us confidence to predict the correlation as it has been described above.

Before we end this section, note that we have chosen to speak in terms of the one- and the two-cycle fixed points only. There are other flux values as well for which one gets different multiple cyclic behavior, even a completely chaotic behavior of the parameter space. All these point toward the existence of extended eigenstates in a 3-simplex network. However, we have tried to focus on a definite correlation between cycles of invariance of the parameter space and a given set of values of the magnetic flux by citing the above example.

VI. CONCLUSION

We have examined the spectral properties of a 3-simplex fractal network in the presence of a magnetic field penetrating a subspace of this fractal space. Both the isotropic and the anisotropic limits of the model have been discussed, with special emphasis on the flux-dependent electronic transmission and the existence of extended electronic states. Based on a numerical study of the exact renormalization group recursion relations we show that there is a subtle correlation between the value of the magnetic flux and the fixed-point behavior of the Hamiltonian, and propose that such an observation may lead to a method of classification of the extended eigenstates for a given value of the energy of the electron.

ACKNOWLEDGMENTS

The author is grateful to the Max Planck Institute für Physik Complexer Systeme, in Dresden for their kind hospitality and for supporting the present work. Special thanks must be given to Magnus Johansson for a critical reading of the manuscript and for valuable comments.

*On leave from Department of Physics, University of Kalyani, Kalyani, West Bengal 741 235, India.

[1] P. W. Anderson, Phys. Rev. **109**, 1492 (1958).
[2] J. B. Sokoloff, Phys. Rep. **126**, 85 (1985).
[3] R. Rammal and G. Toulouse, Phys. Rev. Lett. **49**, 1194 (1982); R. Rammal, J. Phys. (Paris) **45**, 191 (1984).
[4] E. Domany, S. Alexander, D. Bensimon, and L. P. Kadanoff, Phys. Rev. B **28**, 3110 (1983).
[5] W. Schwalm and M. Schwalm, Phys. Rev. B **37**, 5924 (1988).
[6] W. A. Schwalm and M. K. Schwalm, Phys. Rev. B **39**, 12872 (1989).
[7] W. A. Schwalm, M. K. Schwalm, and K. G. Rada, Phys. Rev. B **44**, 382 (1991).
[8] W. A. Schwalm, C. C. Reese, C. J. Wagner, and M. K. Schwalm, Phys. Rev. B **49**, 15650 (1994).
[9] Y.-E. Levy and B. Souillard, Europhys. Lett. **4**, 233 (1987).
[10] A. Aharony, A. B. Harris, and O. Entin-Wohlman, Phys. Rev. Lett. **70**, 4160 (1993).
[11] W. Schwalm and M. Schwalm, in *Fractals in the Natural and Applied Sciences*, ed. by M. Novak (Elsevier, NY, 1994).
[12] B. Mandelbrot, *Fractal Geometry of Nature* (Freeman, San Francisco, 1982).
[13] Y. Gefen, A. Aharony, B. B. Mandelbrot, and S. Kirkpatric, Phys. Rev. Lett. **47**, 1771 (1981).
[14] R. B. Griffiths and M. Kaufman, Phys. Rev. B **26**, 5022 (1982).
[15] W. A. Schwalm and M. K. Schwalm, Europhys. Lett. **10**, 73 (1989).
[16] W. A. Schwalm and M. K. Schwalm, Phys. Rev. B **47**, 7847 (1993).
[17] X. R. Wang, Phys. Rev. B **51**, 9310 (1995).
[18] Arunava Chakrabarti, J. Phys.: Condens. Matter **8**, 7019 (1996); **8**, 10951 (1996).
[19] Arunava Chakrabarti and B. Bhattacharyya, Phys. Rev. B **54**, R12625 (1996).
[20] D. H. Dunlap, H-L. Wu, and P. W. Phillips, Phys. Rev. Lett. **65**, 88 (1990); P. K. Dutta, D. Giri, K. Kundu, Phys. Rev. B **48**, 16347 (1993).
[21] R. Riklund, M. Severin, and Y. Liu, Int. J. Mod. Phys. B **1**, 121 (1987); B. Lindquist, M. Johansson and R. Riklund, Phys. Rev. B **50**, 9860 (1994).
[22] Arunava Chakrabarti, S. N. Karmakar, and R. K. Moitra, Phys. Rev. Lett. **74** 1403 (1995).
[23] A. Chakrabarti and S. N. Karmakar, and R. K. Moitra, Phys. Rev. B **50**, 13276 (1994).
[24] D. Dhar, J. Math. Phys. **18**, 577 (1977); **19**, 5 (1978).
[25] S. Alexander, Phys. Rev. B **29**, 5504 (1984).
[26] J. R. Banavar, L. Kadanoff, and A. M. M. Pruisken, Phys. Rev. B **31**, 1388 (1985).

[27] X. R. Wang, Phys. Rev. B **53**, 012035 (1996).
[28] J. M. Gordon, A. M. Goldman, J. Maps, D. Costello, R. Tiberio, and B. Whitehead, Phys. Rev. Lett. **56**, 2280 (1986).
[29] S. E. Korshunov, R. Meyer, and P. Martinoli, Phys. Rev. B **51**, 5914 (1995).
[30] N. Rabaud, L. Saminadayar, D. Maily, K. Hasselbach, A. Benoit, and B. Etienne, Phys. Rev. Lett. **86**, 3124 (2001).
[31] Arunava Chakrabarti and B. Bhattacharyya, Phys. Rev. B **56**, 13768 (1997); Z. Lin, Y. Cao, Y. Liu, and P. M. Hui, Phys. Rev. B **66**, 045311 (2002).
[32] W. A. Schwalm and B. J. Moritz, Phys. Rev. B **71**, 134207 (2005).
[33] Z. Lin and M. Goda, J. Phys. A **29**, L217 (1996).
[34] B. W. Southern, A. A. Kumar, P. D. Loly, and A. M. S. Tremblay, Phys. Rev. B **27**, 1405 (1983).
[35] A. Adrover, W. Schwalm, M. Giona, and D. Bachand, Phys. Rev. E **55**, 7304 (1997).
[36] M. Hood and B. W. Southern, J. Phys. A **19**, 2679 (1986).
[37] A. D. Stone, J. D. Joannopoulos, and D. J. Chadi, Phys. Rev. B **24**, 5583 (1981).